Journal of Dental Sciences 20 (2025) 2283–2291

Available online at www.sciencedirect.com

ScienceDirect

journal homepage: www.e-jds.com

Original Article

Single-cell isolation reveals 5 fluorouracil-resistant subclones in oral squamous cell carcinoma: New insights into stemness and epithelial–mesenchymal transition for targeted therapies

Wei-Chia Su [a,b,1], Yi-Ming Chang [c,d,1], Hsin-Hu Chen [a], Su-Feng Chen [a], Meng-Hua Yang [d], Yu-Chun Lin [d,e,f], Jian-Hong Yu [a,g*]**

[a] *School of Dentistry, College of Dentistry, China Medical University, Taichung, Taiwan*
[b] *Division of Oral and Maxillofacial Surgery, Department of Dentistry, Ta-Tung Hospital, Kaohsiung, Taiwan*
[c] *Department of Pathology and Laboratory Medicine, Kaohsiung Veterans General Hospital, Kaohsiung, Taiwan*
[d] *Institute of Pathology and Parasitology, National Defense Medical Center, Taipei, Taiwan*
[e] *Graduate Institute of Medical Sciences, National Defense Medical Center, Taipei, Taiwan*
[f] *Department of Pathology, National Defense Medical Center & Tri-Service General Hospital, Taipei, Taiwan*
[g] *Orthodontics, Department of Dentistry, China Medical University Hospital, Taichung, Taiwan*

Received 8 April 2025; Final revision received 27 May 2025
Available online 6 June 2025

KEYWORDS
Resistant subclones;
Cancer stem cells;
Epithelial-mesenchymal transition;

Abstract *Background/purpose:* Oral squamous cell carcinoma (OSCC) often recurs and has poor clinical outcomes, partly attributable to subpopulations that develop resistance to 5 fluorouracil (5FU). Elucidating how these resistant clones emerge and drive tumour aggressiveness is essential for improving OSCC treatment approaches.
Materials and methods: To establish 5FU-resistant cells, SCC25 cells were repeatedly exposed to 5FU, and single-cell clones were subsequently isolated using a microfluidic system. Three

* Corresponding author. School of Dentistry, College of Dentistry, China Medical University, No. 91, Xueshi Road, North District, Taichung, 40402, Taiwan.
** Corresponding author. Department of Pathology, National Defense Medical Center & Tri-Service General Hospital, No.325, Sec.2, Chenggong Rd., Neihu District, Taipei City, 114202, Taiwan.
E-mail addresses: yuchunlin@mail.ndmctsgh.edu.tw (Y.-C. Lin), kenkoyu@mail.cmu.edu.tw (J.-H. Yu).
[1] These authors contributed equally to this work.

https://doi.org/10.1016/j.jds.2025.05.032

Microfluidic single-cell isolation;
3D spheroid culture

subclones-Holoclone, Meroclone, and Paraclone-were evaluated for their 5FU responses, expression of drug-efflux pumps (ABCB1, ABCG2), and resistance in three-dimensional (3D) cultures. Their levels of cancer stem cell (CSC) markers (OCT4, SOX2, CD44, CD133) and epithelial—mesenchymal transition (EMT) markers (E-cadherin, Vimentin, Twist) were also examined. In addition, Transwell assays were performed to assess migration and invasion.
Results: Compared with parental SCC25 cells, the three subclones exhibited markedly higher resistance to 5FU under 3D spheroid conditions, concurrent with upregulated ABCB1 and ABCG2 expression. All three subclones showed enhanced sphere-forming capacity and increased OCT4 and SOX2 levels, consistent with higher proportions of $CD44^{+}/CD133^{+}$ cells. Moreover, Holoclone, Meroclone, and Paraclone each displayed reduced E-cadherin alongside elevated Vimentin, and Twist, characteristic of EMT. Transwell assays confirmed increased migration and invasion, with Holoclone and Paraclone exhibiting particularly pronounced effects.
Conclusion: Extended 5FU treatment in OSCC selects for distinct subclones that exhibit CSC-like traits and EMT-related motility, promoting robust chemoresistance and heightened malignancy. These findings emphasise the importance of developing comprehensive therapeutic strategies that simultaneously target drug-efflux mechanisms, CSC markers, and EMT pathways to more effectively control OSCC progression.

Introduction

Oral squamous cell carcinoma (OSCC) ranks among the most common malignancies of the head and neck, posing a considerable global health burden. Although surgical techniques, radiotherapy, and chemotherapy have evolved, many patients still experience local or distant recurrence.[1,2] 5 fluorouracil (5FU), often in conjunction with other agents such as taxanes, remain a mainstay of OSCC treatment. However, both intrinsic and acquired resistance frequently diminish their effectiveness, leading to suboptimal clinical outcomes.[3,4]

Multiple processes are implicated in chemotherapy resistance. In addition to well-characterised genetic mutations,[5,6] emerging evidence points to non-genetic factors,[7,8] dynamic protein—protein interactions,[9,10] and epithelial—mesenchymal transition (EMT)[11–13] in modulating tumour cell survival under drug-induced stress. This cellular plasticity enables certain subsets of cancer cells to transition between epithelial and mesenchymal states, driving metastasis, cancer stem cell (CSC)-associated stemness, and treatment resistance.[14,15] Notably, CSCs identified by markers such as CD44,[6,16] CD133,[17,18] OCT4,[19,20] and SOX2[21,22] are strongly correlated with therapeutic failure and tumour relapse.[22,23]

In this study, we established a comprehensive platform that integrates microfluidic single-cell isolation,[24–26] three-dimensional (3D) spheroid culture,[9,27,28] and enriched 5FU resistant of SCC25 OSCC cells. We isolated phenotypically distinct subclones-Holoclone, Meroclone, and Paraclone[29,30]-that exhibited differing morphologies and drug sensitivities. We then investigated the expression of drug-efflux transporters (ABCB1, ABCG2),[31] CSC-related markers (OCT4, SOX2, CD44, CD133), and EMT markers (E-cadherin, N-cadherin, Vimentin, Twist). Their migratory and invasive properties were also assessed in vitro.

Our findings underscore the considerable heterogeneity of 5FU-resistant OSCC subclones and the pivotal roles of both CSC-associated and EMT-related pathways in shaping chemotherapy resistance. By focussing on adaptive changes at the single-cell level, this work provides new perspectives for developing targeted therapies that confront not only specific mutations but also the dynamic phenotypic shifts that drive disease progression.

Materials and methods

Cell culture and reagents

SCC25 human OSCC cells (American Type Culture Collection, ATCC) were maintained in Dulbecco's Modified Eagle Medium/Ham's F-12 (DMEM/F-12) supplemented with 10 % foetal bovine serum (FBS) and 1 % penicillin—streptomycin at 37 °C in a 5 % CO_2 atmosphere. Stock solutions of 5 fluorouracil (Sigma—Aldrich, St. Louis, Missouri, USA) were prepared in sterile dimethyl sulphoxide (DMSO). All reagents were of analytical grade.

Generation of 5FU-resistant SCC25 subclone

To emulate clinical chemotherapy regimens more closely, a pulse-exposure approach was adopted. Initially, SCC25 cells were treated with 5FU at its half-maximal inhibitory concentration (IC_{50}) for 24 h, reflecting typical clinical infusion durations. The cells then underwent a 2—3-week recovery period in standard culture conditions, growing to approximately 80 % confluence before the next treatment. This cycle was repeated three times, resulting in a stably 5FU-resistant SCC25 cell population. By mirroring cyclical chemotherapy in patients, this in vitro model provides a more realistic platform for investigating chemoresistance mechanisms and assessing potential therapeutic interventions for oral squamous cell carcinoma.

Single-cell isolation and clonal expansion

A microfluidic-based single-cell sorting device (CellGem®; OriGem Biotech Inc., Taichung, Taiwan) was used to isolate individual cells from the 5FU-resistant SCC25 pool. A suspension of 1×10^6 cells/mL was loaded onto the chip, where microwells facilitated single-cell capture.[26] Excess cells were removed by gentle washing, and the chip was incubated at 37 °C to enable clonal expansion. Over a 10—14 day period, colonies arising from single cells were tracked and categorised according to established keratinocyte-based morphological criteria (Holoclone, Meroclone, Paraclone). Individual clones were then retrieved and cultured further in flasks for downstream analyses.

3D spheroid culture

For three-dimensional growth, we employed a scaffold-free microfluidic system (CellHD256®; OriGem Biotech Inc., Taichung, Taiwan) equipped with microwells. Typically, 1×10^3 cells in 100 μL of medium were dispensed into each well. Following a brief settling period, 450 μL of fresh medium was carefully added, and the chip was placed under standard culture conditions for 96 h to allow spheroid formation. Spheroid size and morphology were examined every 24 h using phase-contrast microscopy.

Reverse-transcription quantitative PCR (RT-qPCR)

Total RNA was extracted using TRIzol reagent (Invitrogen, USA). One microgram of RNA was reverse-transcribed into cDNA (Applied Biosystems, Foster, CA, USA), and RT-qPCR was performed using a SYBR Green detection system on a StepOnePlus Real-Time PCR instrument (Applied Biosystems). GAPDH served as an internal reference. Relative expression levels of ABCB1, ABCG2, OCT4, SOX2, CD44, and CD133 were determined by the ΔΔCt method. Details of primer sequences and reagents are provided in Table 1.

Western blot analysis

Cell lysates were prepared in RIPA buffer and quantified using the bicinchoninic acid (BCA) assay (Thermo Fisher Scientific, Waltham, MA, USA). Equal amounts of protein (30—50 μg) were separated by 8—12 % SDS-PAGE, transferred onto polyvinylidene fluoride (PVDF) membranes, and blocked with 5 % non-fat milk for 1 h. Primary antibodies against ABCB1, ABCG2, OCT4, SOX2, E-cadherin, N-cadherin, Vimentin, and Twist (see Table 2 for details) were applied overnight at 4 °C, followed by incubation with HRP-conjugated secondary antibodies. Signal detection employed an enhanced chemiluminescence substrate, and β-actin was used as the loading control.

Flow cytometry for CSC markers

Subclones were dissociated with trypsin—EDTA, washed in PBS, and adjusted to a concentration of 1×10^6 cells/mL. After blocking in 2 % bovine serum albumin, the cells were incubated with FITC- or PE-conjugated antibodies against CD44 and CD133 (Table 2) for 30 min at 4 °C. Samples were then washed and analysed on a BD FACalibur flow cytometer (BD Biosciences, Milpitas, CA, USA). Data were processed using FlowJo or equivalent software.

Migration and invasion assays

Cell migration and invasion were assessed using Transwell chambers (8-μm pore size; Corning®, NY, USA). For

Table 1 Detailed list of primers used.

Oligo Title	Sequences (5' to 3')	Amplicon Size
GAPDH (Reference Gene)	qFP -AAGGTGAAGGTCGGAGTCAA	314 bp
	qRP -AATGAAGGGGTCATTGATGG	
MDR1	qFP -ATTCCTCGAGAAACTGCGAA	150 bp
	qRP -TCACTTCAGGCAACCAG	
ABCG2	qFP -CTGAGATCCTGAGCCTTTGG	122 bp
	qRP -TGCCCATCACAACATCATCT	
SOX2	qFP -GGCAGCTACGCATGATGCAGGAGC	150 bp
	qRP -CTGGTCATGGAGTTGTACTGCACG	
OCT-4	qFP -CGCACCACTGGCATTGTCAT	247 bp
	qRP -TTCTCCTTGATGTCACGCAC	
E cadherin	qFP - CGCATTGCCACATACACTCT	252 bp
	qRP - TTGGCTGAGGATGGTGTAAG	
Vimentin	qFP - GAGCTGCAGGAGCTGAATG	344 bp
	qRP - GGTCAAGACGTGCCAGAG	
Twist	qFP - ACGAGCTGGACTCCAAGATG	484 bp
	qRP - GGCACGACCTCTTGAGAA TG	

Abbreviation: GAPDH = Glyceraldehyde 3-phosphate dehydrogenase; MDR1 = Multidrug Resistance 1; ABCG2 = ATP binding cassette subfamily G member 2; SOX2 = SRY-Box Transcription Factor 2; OCT-4 = octamer-binding transcription factor 4.

Table 2 Detailed list of primary antibodies used.

Antibody name	Clone	Dilute WB/Flow/IHC	Company
MDR-1	Rabbit pAb (GTX108370)	1:1000	Gene Tex, USA.
ABCG2	Rabbit pAb (GTX100437)	1:1000	Gene Tex, USA.
OCT4	Rabbit pAb (GTX101497)	1:500	Gene Tex, USA.
SOX2	Rabbit pAb (bs0523R)	1:500	Bioss Antibodies, USA.
PE-CD44	Mouse mab (338807)	1:100	BioLegend, USA.
PE-CD133	Mouse mab (393903)	1:50	BioLegend, USA.
E-cadherin	Rabbit pAb (GTX100443)	1:1000/1:300	Gene Tex, USA.
Vimentin	Rabbit pAb (GTX100619)	1:1000/1:500	Gene Tex, USA.
Twist	Rabbit pAb (GTX127310)	1:500	Gene Tex, USA.
b-actin	Mouse mab (ab213262)	1:3000	Abcam, UK

Abbreviation: MDR1 = Multidrug Resistance 1; ABCG2 = ATP binding cassette subfamily G member 2; OCT-4 = octamer-binding transcription factor 4; SOX2 = SRY-Box Transcription Factor 2; PE-CD44 = Phycoerythrin - cluster of differentiation 44; PE-CD133 = Phycoerythrin - cluster of differentiation 133.

migration assays, 1×10^5 cells in serum-free medium were placed in the upper chamber, while the lower chamber was filled with medium containing 10 % FBS as a chemoattractant. After 24 h, non-migratory cells were removed, and cells that had traversed to the underside were fixed, stained with haematoxylin, and counted in five randomly chosen fields. Invasion assays followed a similar protocol but used a 1:2 Matrigel:medium coating on the membrane, with a 24-h incubation. This setup allows straightforward comparisons of each cell population's invasive potential.

Statistical analysis

All data are expressed as mean $\pm$ standard deviation, based on at least three independent experiments. Statistical analyses were conducted using GraphPad Prism (v10, GraphPad Software Inc., La Jolla, CA, USA). Differences between two groups were evaluated with a two-tailed Student's *t*-test, while one-way analysis of variance (ANOVA) with Tukey's post hoc test was used for multiple comparisons. A *P*-value <0.05 was regarded as statistically significant.

Results

Generation and morphological characterisation of 5FU-resistant subclones via microfluidic single-cell isolation

Repeated treatment of SCC25 cells with 5FU at its IC_{50} concentration successfully generated a drug-resistant population, confirming the utility of this selective pressure for modelling therapeutic resistance. Morphologically, these resistant cells differed from their parental counterparts (Fig. 1A), indicative of enhanced migratory or mesenchymal characteristics.

To explore subclonal variation within this resistant population, we employed a microfluidic single-cell isolation platform that allowed individual cells to be cultured in separate microwells under uniform conditions. After 10–14 days, three distinct colony types emerged: Holoclone, Meroclone, and Paraclone (Fig. 1B). Holoclones appeared as densely packed, smooth-edged colonies with high self-renewal potential, whereas Paraclones produced loosely organised, flattened colonies indicative of a more differentiated phenotype. Meroclones combined features of both extremes, forming partially compact and partially dispersed colonies. Thus, prolonged 5FU exposure not only induces widespread chemoresistance but also enriches distinct subpopulations within the same cell line. Furthermore, microfluidic-based single-cell expansion clarifies how heterogeneous responses to 5FU can arise and persist. Identifying these subclones may ultimately guide more targeted therapeutic strategies aimed at eradicating both highly proliferative, stem-like cells and more differentiated populations that drive tumour progression.

Distinct 5FU responses under 3D culture conditions reflect subclonal heterogeneity and drug efflux mechanisms

Next, we investigated multiple drug resistant associated gene and protein. RT-qPCR and Western blotting analyses demonstrated marked upregulation of ABCB1 and ABCG2 in Holoclone and Paraclone (Fig. 2 A and B, $P < 0.01$), highlighting an increased capacity for drug efflux. By contrast, Meroclone exhibited only modest changes in these transporters, implying that alternative mechanisms (e.g., enhanced DNA repair or altered apoptotic pathways) might be at play.

Three-dimensional (3D) spheroid assays revealed that all subclones exhibited greater drug tolerance compared to two-diamensional (2D) cultures (Fig. 2C, $P < 0.01$), underscoring the influence of the microenvironment on chemoresistance. Even so, Holoclone and Paraclone retained notably high viability under drug concentrations that significantly reduced parental spheroid growth, suggesting that their efflux capabilities and/or stem-like features confer substantial resilience. Collectively, these findings emphasise the challenge posed by heterogeneous tumour subpopulations, as they demonstrate distinct survival mechanisms. Furthermore, the discrepancies between 2D and 3D assay outcomes underscore the critical role of tumour architecture in resistance, reinforcing the necessity for combination strategies that target multiple resistance pathways.

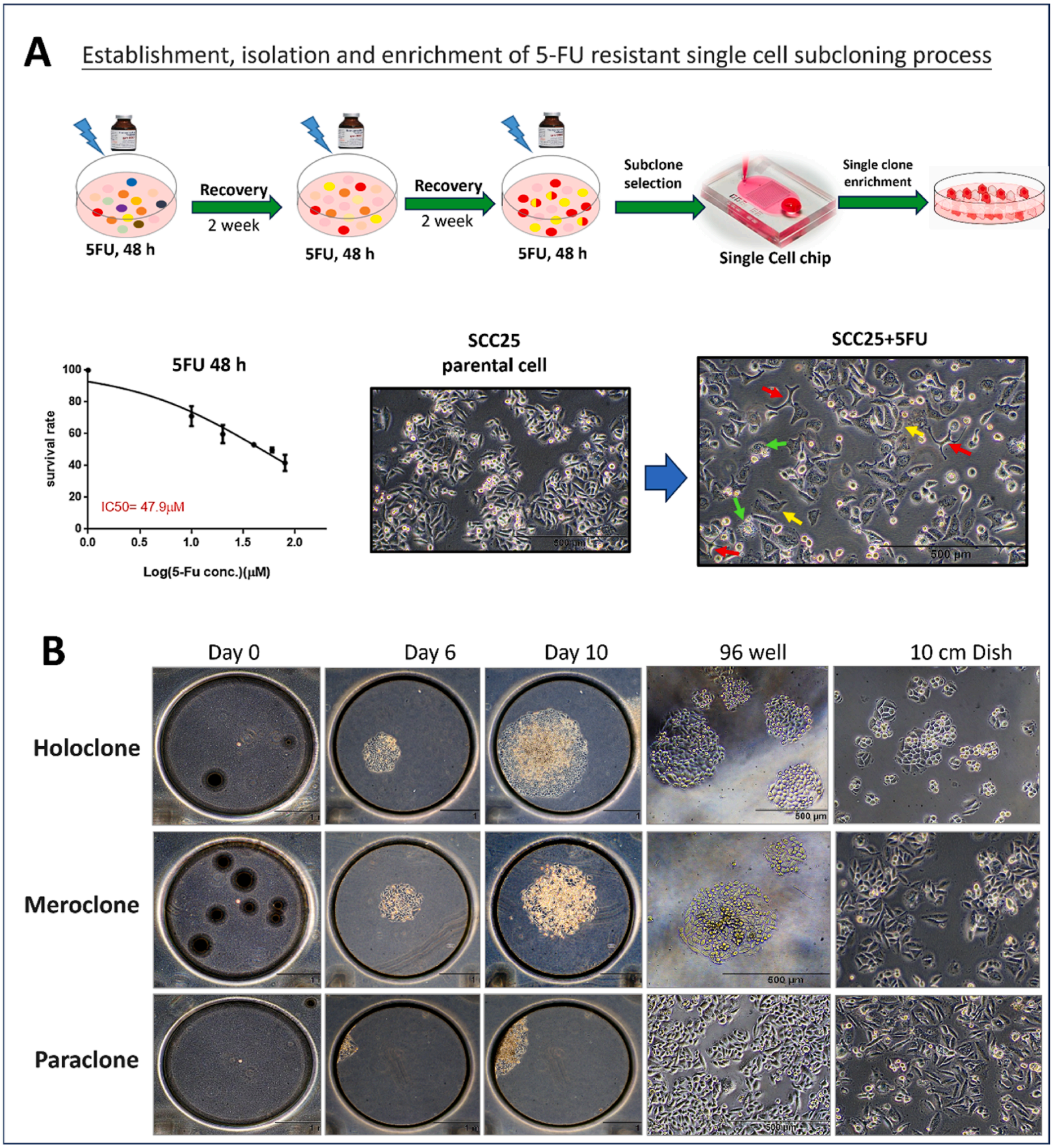

Figure 1 Establishing Drug-Resistant Subclones. Repeated treatment of SCC25 cells with 5FU at IC_{50} concentrations generated a drug-resistant subpopulation characterized by spindle-like (red arrow), irregular (yellow arrow), or round (green arrow) morphologies, in contrast to the parental cells (A). A microfluidic single-cell culture platform was used to isolate individual cells, which were then cultured for 10-14 days. Based on colony morphology, three distinct types emerged: Holoclones (compact colonies with smooth edges and high self-renewal potential), Meroclones (exhibiting both compact and dispersed cell arrangements), and Paraclones (loose, flattened colonies indicative of a more differentiated phenotype) (B). Scale bars 1mm and 500 μm.

Assessment of CSC-like properties in 5FU-resistant OSCC subclones

To elucidate the molecular basis of these cancer stem cell (CSC)-like features, we investigated whether our three subclones possessed such properties. In accordance with the existing literature, which suggests that drug-resistant tumour cells frequently exhibit CSC-like attributes, we performed the expression of the core pluripotency factors SOX2 and OCT4 at both the mRNA and protein levels. Holoclone and Paraclone showed markedly elevated expression of these stemness-related genes, while Meroclone exhibited comparatively lower levels, and the parental SCC25 cells expressed minimal or negligible amounts (Fig. 3A and B, $P < 0.01$).

We further evaluated flow cytometric analysis of the established CSC markers CD133 and CD44 in both the parental SCC25 cells and each subclone. The parental

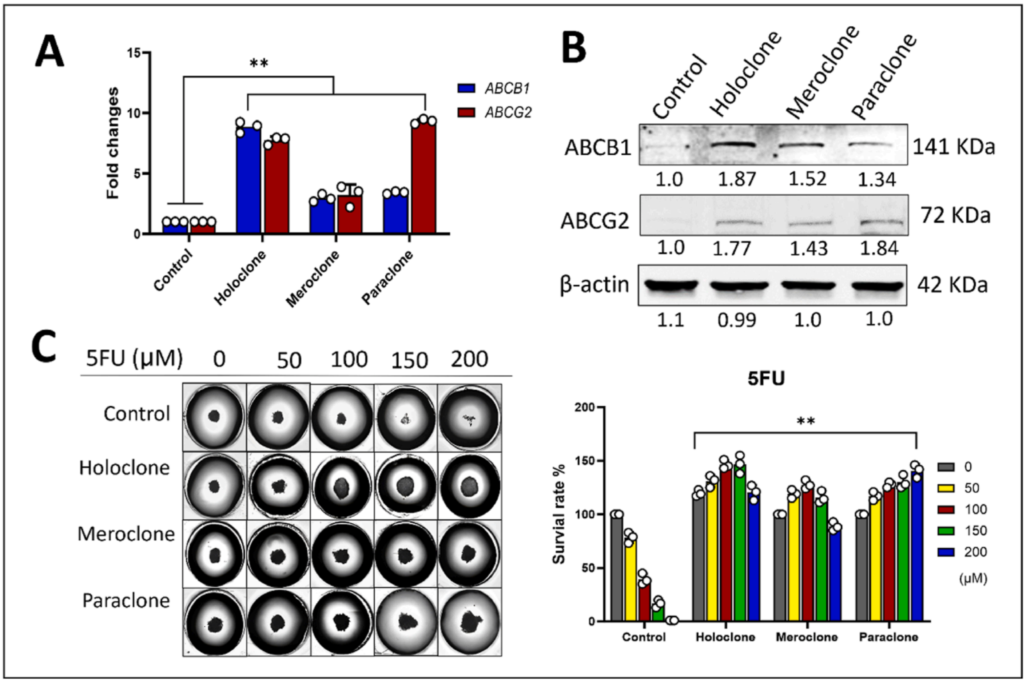

Figure 2 Differences in 5FU resistance markers among subclones. RT-qPCR and Western blot analyses reveal marked upregulation of ABCB1 (P-glycoprotein) and ABCG2 in Holoclone and Paraclone, suggesting enhanced drug efflux capacity (A, B). In three-dimensional (3D) spheroid cultures, all subclones exhibit greater tolerance to 5FU, underscoring the influence of the microenvironment on chemotherapeutic resistance (C). Data are expressed as mean ± SD. White points as sample size; *: $P < 0.05$, **: $P < 0.01$.

SCC25 cells displayed fewer than 50 % CD133^{+}/CD44^{+} populations, whereas all three subclones demonstrated CD133 expression exceeding 99 %. With respect to CD44 levels, Holoclone showed the highest expression, followed by Paraclone and then Meroclone (Fig. 3C). Collectively, these findings confirm that Holoclone and Paraclone harbour stronger CSC-like characterics, underscoring their potential relevance to chemoresistance and tumour progression.

Differential EMT marker expression and increased invasiveness in SCC25 subclones

In this study, we utilised the SCC25 oral squamous cell carcinoma cell line to isolate three distinct subclones-Holoclone, Meroclone, and Paraclone-and investigated the expression of epithelial—mesenchymal transition (EMT) markers (E-cadherin, Vimentin) and the transcription factor Twist. Through RT-qPCR and Western blot analyses, we observed that E-cadherin levels were highest in the parental SCC25 cells, followed by Meroclone, whereas Holoclone and Paraclone both exhibited reduced E-cadherin expression. In contrast, Vimentin was upregulated in Holoclone, Meroclone, and Paraclone, but remained comparatively low in the parental cells. Moreover, Twist expression was most pronounced in Holoclone, moderate in Paraclone, and lower in both the parental SCC25 cells and Meroclone (Fig. 4A and B, $P < 0.01$).

Subsequent migration and invasion assays demonstrated that Holoclone and Paraclone displayed markedly enhanced migratory capacity (Fig. 4C, $P < 0.01$). Taken together, these findings indicate that both Holoclone and Paraclone subclones exhibit stronger EMT characteristics, conferring increased cellular plasticity and more pronounced migratory potential. These results offer valuable insights into the invasive and metastatic behaviours of oral squamous cell carcinoma and may guide the development of future therapeutic strategies.

Discussion

The current study reveals that sustained 5 fluorouracil (5FU) treatment in oral squamous cell carcinoma (OSCC) leads to the emergence of distinct drug-resistant subclones-Holoclone, Meroclone, and Paraclone-with divergent phenotypes, varying degrees of chemotherapy tolerance, and unique molecular profiles. By using a microfluidic-based single-cell isolation method, we were able to separate and expand individual clones, thereby exposing the inherent heterogeneity that underpins chemotherapy resistance in OSCC. Despite focusing on a single OSCC line (SCC25) which may limit broader applicability future investigations incorporating additional lines (e.g., HSC-3, OECM-1) or patient-derived models could still deepen our understanding of 5-FU resistance mechanisms. These findings highlight an important reality in cancer biology: a single cell line can generate multiple subpopulations, each adopting a different strategy for survival under chemotherapeutic pressure.

Our observations corroborate earlier studies showing that repeated drug exposure enriches subpopulations with enhanced drug-efflux mechanisms.[32] Specifically, the upregulation of ABCB1 (P-glycoprotein) and ABCG2 in the most drug-tolerant subclones, Holoclone and Paraclone. We

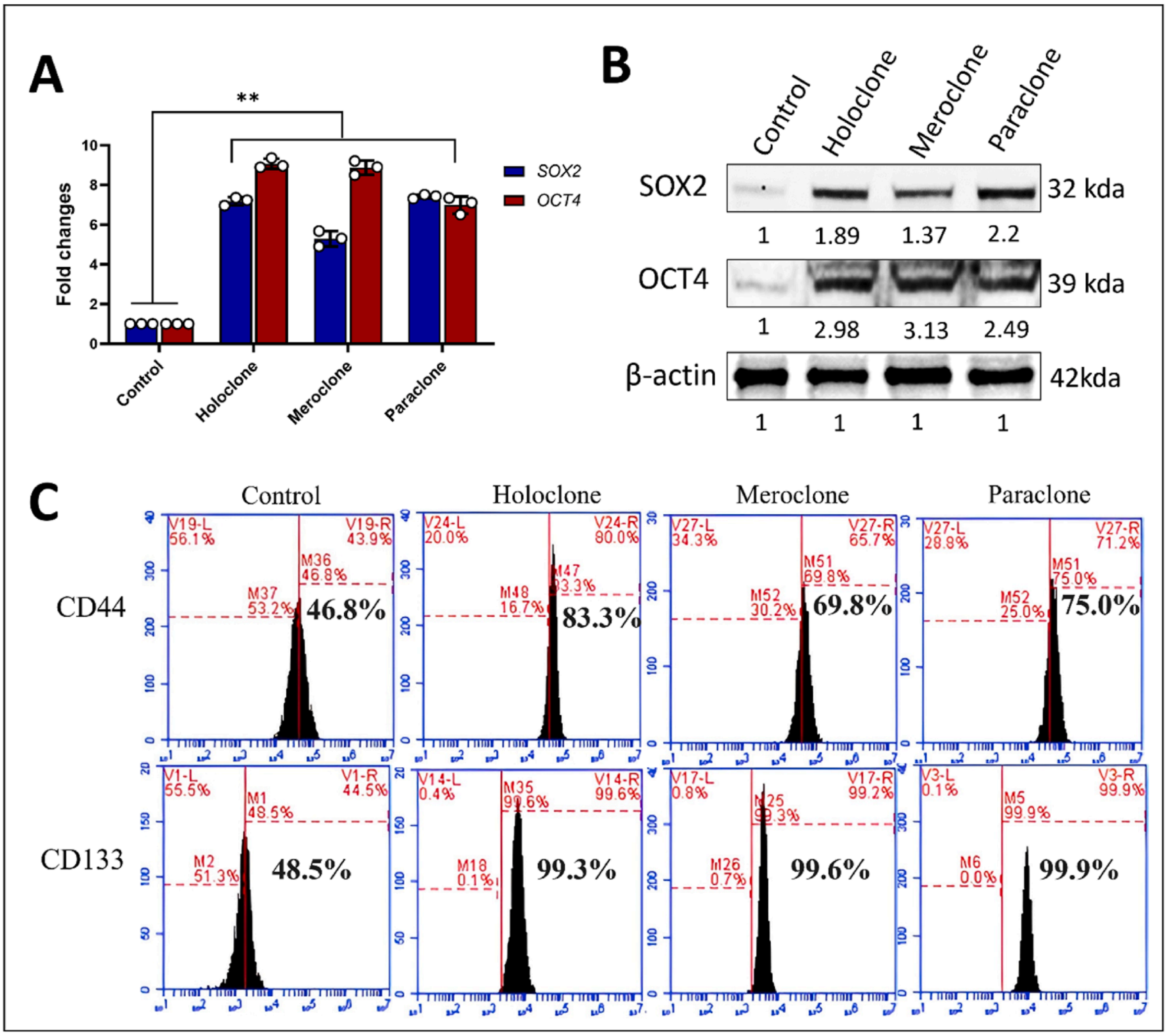

Figure 3 Characterization of CSC-like features in 5FU-resistant OSCC subclones. Analysis of SOX2 and OCT4 at both the mRNA and protein levels shows that Holoclone and Paraclone exhibit markedly elevated expression of these stemness-related factors, whereas Meroclone displays comparatively lower levels and the parental SCC25 cells show minimal or negligible amounts (A, B). Flow cytometric analysis indicates that the parental SCC25 cells have fewer than 50% $CD133^+/CD44^+$ populations, while all three subclones exceed 99% for CD133 expression. Among the subclones, Holoclone exhibits the highest CD44 levels, followed by Paraclone and Meroclone (C). Data are expressed as mean ± SD. White points as sample size; *: $P < 0.05$, **: $P < 0.01$.

maintained the subclones in standard medium (i.e., no 5-FU) for approximately four weeks, during which they generally retained a considerable degree of resistance. Beyond this period, some partial re-sensitization was noted in certain subclones when cultured without drug pressure for an extended duration. This finding aligns with established resistance pathways in various tumor models. Furthermore, three-dimensional (3D) spheroid assays emphasise how the tumour microenvironment can amplify intrinsic resistance, as higher drug tolerance was observed under 3D conditions in all subclones compared with conventional two-dimensional (2D) cultures. These results concur with previous work suggesting that 3D models replicate in vivo drug responses more faithfully, largely due to cell—cell and cell—matrix interactions that modulate survival pathways.[33]

Beyond drug efflux, our data highlight two additional drivers of resistance and aggressiveness: cancer stem cell (CSC)—like properties and epithelial—mesenchymal transition (EMT). Holoclone and Paraclone exhibited increased levels of OCT4 and SOX2, as well as a higher proportion of $CD44^+/CD133^+$ cells-phenotypes frequently linked to enhanced tumour-initiating capacity and resistance to DNA-damaging agents.[34] Concomitantly, downregulation of E-cadherin and upregulation of Vimentin, and Twist in these subclones is indicative of an EMT phenotype, which has been widely associated with metastasis and treatment resistance.[5] Our Transwell assays confirmed that these molecular alterations conferred significantly elevated motility and invasive capabilities, supporting the notion that EMT and CSC traits can synergistically promote more aggressive tumour behaviour.[23,29]

Several important considerations follow from these findings. First, the presence of multiple resistant clones within a single cell line suggests that therapies targeting a single pathway may be insufficient for complete tumour eradication. Second, we highlight the potential cross-talk

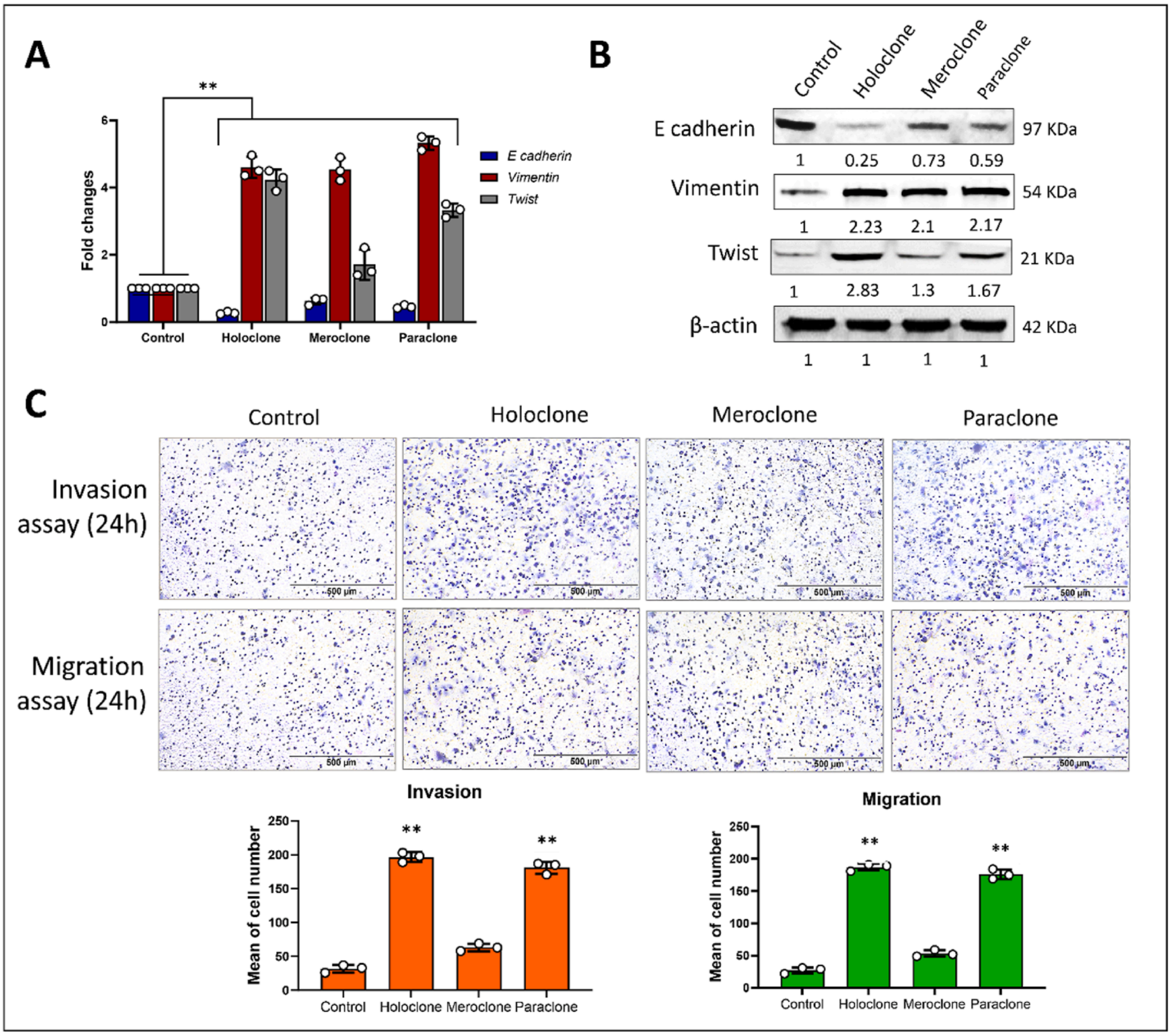

Figure 4 EMT marker profiling and migratory capacity of SCC25-derived subclones. RT-qPCR and Western blot analyses show that the parental SCC25 cells exhibit the highest E-cadherin expression, followed by Meroclone, whereas Holoclone and Paraclone display markedly reduced E-cadherin. In contrast, Vimentin is elevated in all three subclones compared with the parental cells, and Twist is most strongly expressed in Holoclone, moderate in Paraclone, and lower in both parental SCC25 cells and Meroclone (A, B). Transwell-based migration and invasion assays confirm that Holoclone and Paraclone possess significantly enhanced migratory and invasive capacities (C). Scale bars 500 μm. Data are expressed as mean $\pm$ SD. White points as sample size; *: $P < 0.05$, **: $P < 0.01$.

between EMT and CSC pathways, noting in particular how TGF-β, Wnt/β-catenin, and Notch signaling may converge to drive the EMT phenotype and sustain CSC properties in 5-FU-resistant OSCC cells. Furthermore, the strong linkage among CSC-associated traits, drug efflux mechanisms, and EMT underscores the need for combination therapies that simultaneously target stemness signaling, transporter activity, and mesenchymal transformation. Third, our results underscore the value of integrating 3D culture methodologies with single-cell analyses to more accurately capture the complexity of tumour subclones. Incorporating patient-derived specimens into these approaches could further support personalised treatment planning in OSCC.

In conclusion, we show that continuous 5-FU exposure selects for OSCC subclones with robust CSC-like phenotypes, EMT traits, and augmented efflux capacities, collectively driving drug resistance and invasive potential. By elucidating these mechanisms, our study establishes a framework for targeted interventions to overcome 5-FU resistance in OSCC. Pursuing dual-target therapies that combine ABC transporter inhibitors (e.g., ABCG2/ABCB1) with EMT/CSC pathway blockers may reduce chemoresistance and prevent relapse. Furthermore, integrating single-cell isolation and 3D spheroid methods into personalized pipelines could quickly profile patient-derived OSCC cells for resistance patterns and guide combination therapies before clinical administration. Such an approach promises therapeutic outcomes for OSCC.

Declaration of competing interest

The authors have no conflicts of interest relevant to this article.

Acknowledgment

The study was funded by the Tri-Service General Hospital (Grant No. TSGHD-113082). Experiments and data analysis were partly performed using the National Defense Medical Center (Taipei, Taiwan). We would like to thank Ching-Ming Kuo for his technical support throughout the course of this study.

References

1. Li Q, Xia C, Li H, et al. Disparities in 36 cancers across 185 countries: secondary analysis of global cancer statistics. *Front Med* 2024;18:911—20.
2. Bray F, Laversanne M, Sung H, et al. Global cancer statistics 2022: GLOBOCAN estimates of incidence and mortality worldwide for 36 cancers in 185 countries. *CA Cancer J Clin* 2024;74:229—63.
3. Noronha V, Patil V, Chaturvedi P, et al. Phase 3 RCT comparing docetaxel-platinum with docetaxel-platinum-5FU as neo-adjuvant chemotherapy in borderline resectable oral cancer. *Eur J Cancer* 2024;200:113560.
4. Pignon JP, le Maitre A, Maillard E, Bourhis J, Group MNC. Meta-analysis of chemotherapy in head and neck cancer (MACH-NC): an update on 93 randomised trials and 17,346 patients. *Radiother Oncol* 2009;92:4—14.
5. P JN, Patil SR, Veeraraghavan VP, Daniel S, Aileni KR, Karobari MI. Oral cancer stem cells: a comprehensive review of key drivers of treatment resistance and tumor recurrence. *Eur J Pharmacol* 2025;989:177222.
6. Atashi F, Vahed N, Emamverdizadeh P, Fattahi S, Paya L. Drug resistance against 5 fluorouracil and cisplatin in the treatment of head and neck squamous cell carcinoma: a systematic review. *J Dent Res Dent Clin Dent Prospects* 2021;15:219—25.
7. Gupta I, Badrzadeh F, Tsentalovich Y, Gaykalova DA. Connecting the dots: investigating the link between environmental, genetic, and epigenetic influences in metabolomic alterations in oral squamous cell carcinoma. *J Exp Clin Cancer Res* 2024;43:239.
8. Mesgari H, Esmaelian S, Nasiri K, Ghasemzadeh S, Doroudgar P, Payandeh Z. Epigenetic regulation in oral squamous cell carcinoma microenvironment: a comprehensive review. *Cancers (Basel)* 2023;15:5600.
9. Sun J, Skanata A, Movileanu L. Single-molecule observation of competitive protein-protein interactions utilizing a nanopore. *ACS Nano* 2025;19:103—15.
10. Ali M, Zhang Z, Ibrahim MAA, Soliman MES. Heat shock protein (Hsp27)-ceramide synthase (Cers1) protein-protein interactions provide a new avenue for unexplored anti-cancer mechanism and therapy. *J Recept Signal Transduct Res* 2024;44:41—53.
11. Gupta S, Silveira DA, Lorenzoni PR, Mombach JCM, Hashimoto RF. LncRNA PTENP1/miR-21/PTEN axis modulates EMT and drug resistance in cancer: dynamic boolean modeling for cell fates in DNA damage response. *Int J Mol Sci* 2024;25:8264.
12. Feng Q, Yang P, Wang H, et al. ID09, A newly-designed tubulin inhibitor, regulating the proliferation, migration, emt process and apoptosis of oral squamous cell carcinoma. *Int J Biol Sci* 2022;18:473—90.
13. Hamoui MZ, Rizvi S, Arnouk H, Roberts CM. Putative biomarkers for prognosis, epithelial-to-mesenchymal transition, and drug response in cell lines representing oral squamous cell carcinoma progression. *Genes* 2025;16:209.
14. Acharya SK, Shai S, Choon YF, et al. Cancer stem cells in oral squamous cell carcinoma: a narrative review on experimental characteristics and methodological challenges. *Biomedicines* 2024;12:2111.
15. Biddle A, Gammon L, Liang X, Costea DE, Mackenzie IC. Phenotypic plasticity determines cancer stem cell therapeutic resistance in oral squamous cell carcinoma. *EBioMedicine* 2016;4:138—45.
16. Tandon A, Singh NN, Gulati N. CD44 related stemness maneuvers oral squamous cell carcinoma biology. *Indian J Pathol Microbiol* 2022;65:268—73.
17. Wen XT, Ma Z, Zhang C, Tao SC, Chen XJ, Mai HM. Maintenance of the stemness in CD133(+)primary oral squamous cell carcinoma cells under different culture conditions. *Shang Hai Kou Qiang Yi Xue* 2022;31:343—8.
18. Ma Z, Zhang C, Liu X, et al. Characterisation of a subpopulation of CD133(+) cancer stem cells from Chinese patients with oral squamous cell carcinoma. *Sci Rep* 2020;10:8875.
19. Dai Y, Wu Z, Chen Y, Ye X, Wang C, Zhu H. OCT4's role and mechanism underlying oral squamous cell carcinoma. *J Zhejiang Univ - Sci B* 2023;24:796—806.
20. Sun S, Yang H, Wang F, Zhao S. Oct4 downregulation-induced inflammation increases the migration and invasion rate of oral squamous cell carcinoma. *Acta Biochim Biophys Sin* 2021; 53:1440—9.
21. Sacco A, Battaglia AM, Santamaria G, et al. SOX2 promotes a cancer stem cell-like phenotype and local spreading in oral squamous cell carcinoma. *PLoS One* 2023;18:e0293475.
22. Rizzo D, Graziani C, Gallus R, et al. Stem cell markers in oral and oropharyngeal squamous cell carcinomas in relation to the site of origin and HPV infection: clinical implications. *Acta Otorhinolaryngol Ital* 2020;40:90—8.
23. Tokozlu B, Yucel OO, Gultekin SE, Bozdag LA. Epithelial mesenchymal transition and cancer stem cell markers in oral epithelial dysplasia and oral squamous cell carcinoma. *Pol J Pathol* 2024;75:305—14.
24. Wang C, Qiu J, Liu M, et al. Microfluidic biochips for single-cell isolation and single-cell analysis of multiomics and exosomes. *Adv Sci (Weinh)* 2024;11:e2401263.
25. Hochstetter A. Lab-on-a-chip technologies for the single cell level: separation, analysis, and diagnostics. *Micromachines (Basel)* 2020;11:468.
26. Chen HH, Nguyen TV, Shih YH, et al. Combining microfluidic chip and low-attachment culture devices to isolate oral cancer stem cells. *J Dent Sci* 2024;19:560—7.
27. Chen Z, Park S. Three-dimensional hanging drop spheroid plates for easy chimeric antigen receptor (car) t cytotoxicity assay. *Methods Mol Biol* 2024;2764:35—42.
28. Rasouli M, Safari F, Kanani MH, Ahvati H. Principles of hanging drop method (spheroid formation) in cell culture. *Methods Mol Biol* 2025;2879:289—300.
29. Tieche CC, Gao Y, Buhrer ED, et al. Tumor initiation capacity and therapy resistance are differential features of emt-related subpopulations in the nsclc cell line a549. *Neoplasia (New York, N Y)* 2019;21:185—96.
30. Chen SH, Yu JH, Lin YC, Chang YM, Liu NT, Chen SF. Application of an integrated single-cell and three-dimensional spheroid culture platform for investigating drug resistance heterogeneity and epithelial-mesenchymal transition (EMT) in lung cancer subclones. *Int J Mol Sci* 2025;26:1766.
31. Lu X, Wang Z, Huang H, Wang H. Hedgehog signaling promotes multidrug resistance by regulation of ABC transporters in oral squamous cell carcinoma. *J Oral Pathol Med* 2020;49:897—906.
32. Wang S, Wang SQ, Chen XB, et al. Cell-based screen identifies a highly potent and orally available abcb1 modulator for treatment of multidrug resistance. *J Med Chem* 2024;67:18764—80.
33. Bhuker S, Sinha AK, Arora A, et al. Genes and proteins expression profile of 2D vs 3D cancer models: a comparative analysis for better tumor insights. *Cytotechnology* 2025;77:51.
34. Adnan Y, Ali SMA, Farooqui HA, Kayani HA, Idrees R, Awan MS. High CD44 immunoexpression correlates with poor overall survival: assessing the role of cancer stem cell markers in oral squamous cell carcinoma patients from the high-risk population of Pakistan. *Int J Surg Oncol* 2022;2022:9990489.